Research Square

Preprints are preliminary reports that have not undergone peer review.
They should not be considered conclusive, used to inform clinical practice,
or referenced by the media as validated information.

Phase closure in three dimensions and electromagnetic coupling

Artur Novais

arturnovais@gmail.com

Universidade Estadual de Santa Cruz

Research Article

Keywords: Fine structure constant, Phase closure, Quantum-relativistic geometry, Geometric regulators

Posted Date: August 10th, 2026

DOI: https://doi.org/10.21203/rs.3.rs-10060472/v1

License: This work is licensed under a Creative Commons Attribution 4.0 International License.
Read Full License

Additional Declarations: No competing interests reported.

Phase closure in three dimensions and electromagnetic coupling

Artur Novais

Laboratório de Astrofísica Teórica e Observacional, Universidade Estadual de Santa Cruz, Ilhéus, 45662-900, Brasil.

Contributing authors: arturnovais@gmail.com;

Abstract

We propose a three-dimensional definition of phase closure based on a geometric consistency condition linking 2D phase closure to 3D mode overlap for two intersecting spheres. The spheres represent the relational limits of quantum-phase influence, with radii set by the two-body separation alone. Imposing that a relativistic two-dimensional phase invariant equals the ratio of total to interacting modes in the 3D geometry yields, at tree level, a parameter-free constraint whose only geometrically admissible solution is $\boldsymbol{\alpha_1^{-1} = 137.190}$, within **0.11%** of the observed fine structure constant and obtained independently of any assumed value or dynamical property. Higher-order geometric corrections with coefficients fixed by the same two-sphere geometry give $\boldsymbol{\alpha^{-1} = 137.035999177}$ through fourth order, agreeing at the $\boldsymbol{0.7\sigma}$ level with the determination of $\boldsymbol{\alpha}$ from the electron magnetic moment ($\boldsymbol{g-2}$), the most precise value independent of the atomic-recoil measurements. The construction is not derived from QED and reproduces the Schwinger term $\boldsymbol{a_e = \alpha/2\pi}$ as an additional consistency check. The fifth-order term produces a two-tier prediction: at $\boldsymbol{10^{-9}}$ absolute uncertainty, the series requires $\boldsymbol{\alpha^{-1} = 137.035999177(5)}$; at $\boldsymbol{10^{-10}}$ resolution, it predicts $\boldsymbol{\alpha^{-1} = 137.0359991768(5)}$. Values outside either interval would falsify the series at the respective precision. This provides a direct experimental test of whether electromagnetic coupling is constrained by geometric phase coherence in three dimensions.

Keywords: Fine structure constant, Phase closure, Quantum-relativistic geometry, Geometric regulators

1 Introduction

Among the dimensionless parameters of fundamental physics, none has sparked more sustained fascination than the fine structure constant,

$$\alpha = \frac{e^2}{4\pi\varepsilon_0\hbar c} \simeq \frac{1}{137.036}, \tag{1}$$

which governs the strength of electromagnetic interactions. Its numerical value is experimentally known to extraordinary precision, yet its theoretical origin and specific magnitude remain unexplained. This tension between empirical exactness and conceptual opacity has persisted throughout the twentieth century and continues to motivate foundational inquiry.

The quest for the origin of the fine structure constant is nearly as old as quantum theory itself. It first appeared in 1916 through Arnold Sommerfeld's relativistic extension of Bohr's atomic model (Bohr 1913; Sommerfeld 1916). By incorporating elliptical orbits and relativistic corrections to electron motion, Sommerfeld accounted for the observed splitting of hydrogen spectral lines, the "fine structure", and identified a dimensionless parameter measuring the relativistic strength of electromagnetic coupling. The emergence of such a pure number, independent of units and scales, was immediately striking. Sommerfeld himself emphasized that his theory represented a confluence of the then-nascent electron theory, quantum theory, and special relativity.

Einstein quickly grasped the conceptual importance of dimensionless constants, repeatedly stressing that a genuine understanding of fundamental physics should ultimately explain them rather than simply accommodate them empirically (Einstein 1949). This perspective foreshadowed the century-long expectation that the fine structure constant might one day be calculable from first principles, perhaps within a unified theory of interactions.

Wolfgang Pauli articulated this unease with characteristic emphasis. In correspondence and lectures over several decades, Pauli reiterated the "double mystery" of the fine structure constant, both its numerical value and its universal role across atomic, relativistic, and quantum phenomena (Pauli 1946, 1955).

With the development of relativistic quantum mechanics and quantum electrodynamics (QED), the status of α evolved. In Dirac's theory it appears as the natural expansion parameter controlling relativistic corrections, while in QED it governs the perturbative series underlying radiative corrections and renormalization (Dirac 1928). Precision tests of QED, such as the anomalous magnetic moment of the electron and atomic recoil, have provided some of the most accurate determinations of α (Hanneke et al. 2008; Mohr et al. 2016; Parker et al. 2018; Morel et al. 2020; Fan et al. 2023; Tiesinga et al. 2024). However, these successes did not solve the conceptual puzzle: QED presupposes the value of α but does not predict it.

The renormalization program of QED introduced a new layer to the discussion. The observed value of α depends on energy scale through vacuum polarization, becoming a running coupling constant in the language of quantum field theory (Gell-Mann and Low 1954). Nonetheless, the low-energy limit relevant for atomic physics remains anchored near $1/137$, and the renormalization group flow itself requires a boundary

condition, again leaving the fundamental origin of the value unaddressed (Weinberg 1989, 2007).

Richard Feynman famously highlighted this point in his lectures on QED, describing the fine structure constant as a number "that comes to us with no understanding by man" (Feynman 1985). Feynman's emphasis was not on dissatisfaction with QED's predictive power, but on the stark contrast between computational mastery and conceptual ignorance. His remarks crystallized a widely shared sentiment among mid-century physicists.

In parallel with physical developments, multiple speculative frameworks sought to derive α from numerological considerations. The first example comes from the early ideas of Eddington, who argued on cosmological and combinatorial grounds that α^{-1} should equal an exact integer, originally 136 and later revised to 137 (Eddington 1931, 1936). But perhaps the most prominent of these mathematical enterprises was Armand Wyler's proposal in 1969, which expressed α in terms of volumes of certain symmetric spaces associated with conformal groups (Wyler 1969). Interestingly, Wyler's formula reproduced the experimental value to within parts per million. This coincidence generated intense interest and scrutiny. Subsequent analyses, however, revealed that Wyler's derivation relied on ad hoc identifications and lacked a compelling physical justification. Although the numerical agreement was intriguing, it is now widely regarded as accidental (Robertson 1971; Adler 1972).

Contemporary reviews continue to stress that, despite extraordinary progress in precision measurement and quantum field theory, there is no consensual derivation from first principles, emphasizing the recurring tension between physical explanation and mathematical pattern-finding (Kragh 2003; Jentschura and Nándori 2014; Bronnikov et al. 2025).

The history of the fine structure constant throughout the twentieth century unfolded alongside major breakthroughs in theoretical physics, from atomic models and relativity, through quantum electrodynamics, to modern field theory, while the discovery of its own foundations remained elusive.

2 The nature of a satisfactory answer

Before proceeding to a proposed solution, it is necessary to clarify what is meant by a satisfactory answer to the question "Why is $\alpha^{-1} \simeq 137$?"

This challenge is often posed as if a deeper theoretical embedding of α would suffice. However, the twentieth century literature demonstrates that many attempted explanations through extra associations, while suggestive, ultimately fail to close the explanatory gap they seek to address.

It is well established that the fine structure constant appears ubiquitously throughout physical theory: in atomic spectra and relativistic corrections (Sommerfeld 1916); in QED, setting the probability amplitude for an electron to emit or absorb a photon (Dirac 1928; Feynman 1985) and playing a central role in calculating the anomalous magnetic dipole moment of the electron (Schwinger 1948); in renormalization group flows as a scale-dependent effective coupling (Gell-Mann and Low 1954), and many

other examples. To illustrate this ubiquity, Eq. (2) shows that α can be expressed through a variety of physical relations:

$$\alpha = \frac{v_e}{c} = \frac{\hbar}{m_e c a_0} = \sqrt{\frac{2|E_1|}{m_e c^2}} = \frac{r_e}{\lambda_C} = \frac{\lambda_C}{2\pi a_0}. \tag{2}$$

These expressions identify α from the following perspectives: the ratio of the velocity of the electron in the first Bohr orbit to the speed of light (Sommerfeld 1916); the ratio of the reduced Planck constant to the product of the electron's rest mass, the speed of light, and the Bohr radius (a_0), representing the scale of atomic structures (Griffiths and Schroeter 2018); the square root of the ratio between the ground-state binding energy of the electron and its relativistic rest mass energy (Sommerfeld 1923); and the ratio of the classical electron radius (r_e) to the reduced Compton wavelength (λ_C), or similarly, the ratio of λ_C to the circumference of the first Bohr orbit ($2\pi a_0$) (Jackson 1999).

All these formulae describe how α appears within established frameworks but do not provide a theoretical derivation of its specific dimensionless value. In contemplating this multiplicity of fundamental ratios, it becomes evident that a final answer cannot simply be the discovery of yet another identity involving physical constants.

One may even push this exercise to far-reaching limits and envision speculative discoveries, for instance, that α^{-1} corresponds to the number of spacetime degrees of freedom in a higher-dimensional theory or that it encodes a characteristic imprint of quantum gravity at the earliest moments of cosmological evolution, all described by an elegant relation that involves the gravitational constant G. However, even such spectacular findings would merely relocate, rather than resolve, the problem. One is promptly compelled to ask why this particular number arises. Why do all these impressive relations converge to the pure quantity $\alpha^{-1} \simeq 137$, rather than 42, $50\sqrt{2}$, 1000, or any other specific value?

Pointing to yet another elegant combination of fundamental constants would not get to the bottom of the riddle.

There exists, however, a class of explanations in physics and mathematics that are widely regarded as satisfactory in a much stronger sense: geometric explanations. When one asks why π equals $3.14159\ldots$, or why the diagonal of a unit square equals $\sqrt{2}$, no further "why" is demanded once the axioms of Euclidean geometry are accepted. These numbers are not adjustable parameters or empirical inputs; they are necessary consequences of geometric structure (Heath 1956). Their acceptance as irreducible facts means that geometry itself provides both their definition and their inevitability.

A genuinely satisfactory answer for the fine structure constant must meet this same standard. The value $\alpha^{-1} \simeq 137$ must arise unavoidably from a well-defined geometric construction, not as a fitted parameter, boundary condition, or result of dynamical evolution contingent upon prior choices. In such a framework, the question "why this value?" would be rendered as misplaced as asking why the ratio of a circumference to the diameter equals π. The number would simply be what the geometry enforces.

At first sight, this requirement appears to be implausibly strong. Geometry is traditionally associated with numbers of order unity, such as π, $\sqrt{2}$ and $\sqrt{3}$. By contrast,

the fine structure constant is parametrically small, with $\alpha \sim 10^{-2}$. This disparity has long contributed to the argument that α must be fundamentally dynamical, environmental, or anthropic in origin (Barrow and Tipler 1986). It also helps explain why a geometric interpretation remained elusive for more than a century.

However, this objection is not decisive. Geometry is not intrinsically limited to producing dimensionless numbers of order unity. Manifold constructions in higher-dimensional spaces and nontrivial symmetry reductions can generate small or large pure numbers without invoking tunable parameters (Candelas et al. 1985; Lang 1988). More importantly, we are far from exhausting even the simplest geometric possibilities. The historical difficulty may therefore reflect limitations in the geometric frameworks explored, rather than a fundamental impossibility.

From this perspective, the puzzle of the fine structure constant becomes more sharply formulated. The challenge is not simply to relate α to known physical quantities, nor even to embed it within a unified dynamical theory, but to identify a geometric principle from which its numerical value follows by necessity. Only such an explanation can truncate the infinite regress of "why" questions that has accompanied the constant since its introduction.

If the fine structure constant is to be understood in the same conceptual category as π or $\sqrt{2}$, then its explanation must ultimately be geometric or contained within the geometric core of physical models. The remainder of this work proceeds under this guiding principle.

3 Phase closure in two and three dimensions

A recurring theme in the long history of attempts to understand the fine structure constant is the persistent appearance of π, emerging repeatedly at the boundary between serious physical reasoning and more speculative numerological efforts. From the early days of quantum theory, π entered naturally through the quantization of angular momentum, where circular motion and phase closure impose intrinsic geometric constraints. It is not surprising then that many approaches have assumed that a fundamental explanation of α would ultimately involve π. In this section, we show that this instinct was indeed well motivated.

Furthermore, the present geometric construction does not merely display π as an incidental numerical factor in a final expression; rather, π provides the structural backbone of the derivation. It first appears as the quantum ruler that dictates the ratio of the wavelength to the diameter, being consistently promoted to a relativistic form. Subsequently, π reappears as a volumetric ratio under a three-dimensional phase-closure condition.

These two roles are not independent: the relativistic version of π acts as a cross-dimensional invariant, defining the mode-counting ratio that must be achieved in the interactive volumetric sector. Only then does the output reveal itself: the fine structure constant is numerically equivalent to a geometric constraint that reconciles two manifestations of π, once the proposed definition of 3D phase closure is accepted and built upon.

3.1 Targeted review of 2D phase closure

We start our geometric development by invoking a two-dimensional picture of an electron surrounded by a geometric locus of radius R. Classically, this corresponds to a perfect circle, but in quantum mechanics, this boundary cannot be infinitely sharp. It must be of probabilistic nature, and the probability wave around the circumference must exhibit perfect phase closure ($\lambda = 2\pi R$), which may manifest itself in a physical interaction as the quantization of angular momentum,

$$mv\lambda = h \implies mv(2\pi R) = h \implies mvR = \hbar \implies L = \hbar. \tag{3}$$

A key distinction of our geometric exploration is its focus on the amplitude of the wave, since it will be directly related to the uncertainty in the interaction's separation. In Figure 1, we unwrap the circle to focus on the oscillation around the classical circumference. A useful way to analyze the plane wave is to attribute it to uncertainty in the radial velocity $\Delta\dot{r}$, which cannot be perfectly constrained to zero in a quantum setting.

Our frame is one that keeps the perimeter $2\pi R$ as the length of the wavy path such that the oscillation period is preserved as the perimeter divided by the orbital velocity ($T = 2\pi R/v$). Thus, the amplitude is given by the contribution of the radial velocity multiplied by one-fourth of the period ($A = \Delta\dot{r}T/4$). When $\Delta\dot{r} \ll v$, yielding $A \ll R$, the path length can be evaluated through the red lines, and the perimeter of the classical circle has to be transformed to conform to this reference frame, turning into P', which can be calculated via the Pythagorean relation

$$(P'/4)^2 + (\Delta\dot{r}T/4)^2 = (P/4)^2 \tag{4}$$

$$(2\pi' R)^2 + \left(\frac{\Delta\dot{r}2\pi R}{v}\right)^2 = (2\pi R)^2 \tag{5}$$

$$\pi' = \pi\sqrt{1 - \left(\frac{\Delta\dot{r}}{v}\right)^2}. \tag{6}$$

Here we can label the dimensionless scaling $\Delta\dot{r}/v$ as a generic α,

$$\pi' = \pi\sqrt{1 - \alpha^2}, \tag{7}$$

which is an effective incarnation of π encapsulating the geometry of a wave around a circumference that is subject to phase closure.

Note that to make this transformation Lorentz-invariant, $\Delta\dot{r}/v$ must equal v/c. Although we derived a generalized case, when Lorentz-invariance enters, this turns out to be the scaling of the most relevant example of 2D phase closure: the ground state of the Bohr model,

$$\frac{\Delta\dot{r}}{v} = \frac{v}{c} = \alpha. \tag{8}$$

This is but a first indication that the generic α may indeed be associated with the electromagnetic coupling constant and that π' is the consistent promotion of π

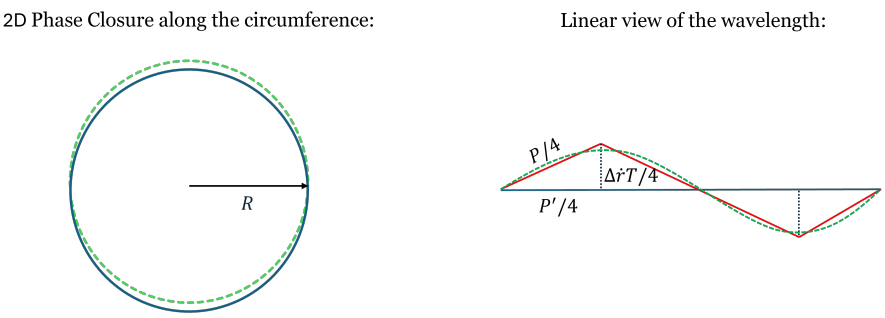


Fig. 1 2D phase closure. The classical circumference $2\pi R$ is modified by radial uncertainty $\Delta\dot{r}$, yielding effective π' and amplitude A.

to a quantum-relativistic form. However, we proceed to the 3D construction without inserting any a-priori value or coupling property. Whether this correspondence is numerically valid is for the geometric consistency to decide.

Finally, closing the 2D analysis, the amplitude of the plane wave is

$$A = \Delta\dot{r}T/4 = \frac{\Delta\dot{r}}{v}\frac{2\pi R}{4} \tag{9}$$

$$A = \frac{\alpha\pi R}{2}. \tag{10}$$

Nothing in this review of 2D phase closure is novel. We simply expressed the effective perimeter and the amplitude of the wave as a function of $\Delta\dot{r}/v$, labeled as a generic α. The novelty comes next, when a definition of 3D phase closure is motivated and postulated.

3.2 Three-dimensional phase closure and projection of the 2D amplitude

We now extend the two-dimensional phase-closure picture to three dimensions. Consider two electrons separated by a distance d. To each electron we attribute a spherical region of quantum-phase influence centered at the particle's position. Among all possible assignments of radius R to each sphere, the condition $R = d$ is the unique scale-invariant choice: it couples spatial extent directly to separation without introducing an independent length scale. Any other ratio R/d would itself be a dimensionless parameter—precisely what the construction aims to derive rather than assume. We therefore associate with each electron a sphere of radius $R = d$, representing the geometric locus where its phase is defined. These spheres do not represent fixed physical boundaries, but rather the relational limits of quantum-phase influence: geometric loci whose extent is set entirely by the two-body separation d, providing a natural spatial scale at which phase coherence between the two electrons is localized. The classical intersection of these spheres is a lens whose volume quantifies the spatial region of mutual influence.

The volume of a spherical lens with separation $s = d/R$ is given by

$$V_{sphere} = \frac{4}{3}\pi R^3; \qquad V_{lens} = \frac{\pi R^3}{12}(4+s)(2-s)^2. \tag{11}$$

Thus, the volumetric ratio is

$$\frac{V_{sphere}}{V_{lens}} = \frac{16}{(4+s)(2-s)^2}. \tag{12}$$

Since the distance equals the radii of the spheres ($s = 1$), we can calculate the ratio in the classical case (perfectly defined positions and distances):

$$\left(\frac{V_{sphere}}{V_{lens}}\right)_{Classical} = \frac{16}{5} = 3.2. \tag{13}$$

Quantum mechanically, however, the spherical boundaries cannot be infinitely sharp. The 2D derivation establishes the amplitude scaling $A = \alpha\pi R/2$, using the peak radial excursion as a simplifying device. This scaling carries forward into the 3D calculation; the physically appropriate boundary displacement is the time-averaged quantity derived below, which uses the root mean square (rms) of the sinusoidal projection rather than the instantaneous peak. In three dimensions, the oscillation plane has one rotational degree of freedom relative to $\hat{z}$, parameterized by the angle $\theta \in [0, \pi]$ between the plane normal and $\hat{z}$, with uniform measure $d\theta/\pi$. Since an in-plane vector is orthogonal to the normal, its projection onto $\hat{z}$ scales as $\sin\theta$: when $\theta = 0$ the plane is perpendicular to $\hat{z}$ and the projection vanishes; when $\theta = \pi/2$ the plane contains $\hat{z}$ and the projection is maximal. The boundary displacement is a static quantity set by the time-averaged reach of the oscillation over one cycle. The projection of circular motion onto any fixed axis is sinusoidal: if the orbit lies in a plane tilted at angle θ to $\hat{z}$, the z-component of the orbital displacement is $A\sin\theta\cos(\omega t)$, which has rms $A\sin\theta/\sqrt{2}$. The tilt angle is uniformly distributed over $[0, \pi]$ with normalized measure $d\theta/\pi$, since it represents a single rotational degree of freedom with no preferred orientation. Combining the rms amplitude with the tilt average gives the effective boundary displacement:

$$A' = \frac{1}{\pi}\int_0^\pi \frac{A\sin\theta}{\sqrt{2}}\, d\theta = \frac{A}{\sqrt{2}} \cdot \frac{2}{\pi} = \frac{\sqrt{2}\,A}{\pi}. \tag{14}$$

Substituting $A = \alpha\pi R/2$ from Eq. (10):

$$A' = \frac{\sqrt{2}}{\pi} \cdot \frac{\alpha\pi R}{2} = \frac{\alpha R}{\sqrt{2}}. \tag{15}$$

Each sphere's boundary is displaced inward by A', so the centers are effectively closer by $2A'$. The dimensionless separation becomes

$$s = \frac{d - 2A'}{R} = 1 - \frac{2A'}{R} = 1 - \sqrt{2}\alpha \equiv 1 - \delta s_1, \tag{16}$$

with

$$\delta s_1 = \sqrt{2}\alpha, \tag{17}$$

and the new volumetric ratio is given by

$$\frac{V_{sphere}}{V_{lens}} = \frac{16}{(5-\sqrt{2}\alpha)(1+\sqrt{2}\alpha)^2}. \tag{18}$$

Finally, to extend the 2D framework to the 3D picture, we need a three-dimensional definition for phase closure. In two dimensions, phase closure for a circular geometric locus is expressed by the identity $\lambda/D = \pi$, where λ is the wavelength and $D = 2R$ is the diameter. The latent periodicity of the wave, λ, spans the realized spatial extent of one interaction cycle, D. The frame that preserves the period, which is essential in the context of quantized energy, gives the invariant ratio $\pi' = \pi\sqrt{1-\alpha^2}$. If $\alpha \triangleq \Delta\dot{r}/v = 2A/\pi R$ is then identified with v/c, the quantum picture is also consistently promoted to relativistic kinematics and the spatial extent is Lorentz-contracted. Thus, π' is the unique dimensionless number that reconciles wave periodicity with relativistic propagation in 2D.

To generalize to three dimensions we promote the 2D picture to a mode-counting statement. In 2D, the orbit supports one family of standing-wave modes; the condition $\lambda/D = \pi$ selects the subset of modes that close phase after one revolution. In 3D, each electron possesses a complete spectrum of spherical standing-wave modes filling its sphere of radius R. The sphere represents the total latent mode space available to one electron before interaction; its volume measures the number of orthogonal 3D modes compatible with boundary conditions at radius R.

When two spheres intersect, only the subset of modes that are simultaneously eigenmodes of both spheres can mediate the interaction. That subset is defined by the intersection lens; its volume, therefore, measures the number of shared modes, i.e. the realized degrees of freedom of the two-body phase coupling. Modes in the non-overlapping regions remain latent for each electron individually but do not contribute to mutual phase closure.

Phase closure in 3D therefore may be defined by the identity between the ratio of total to interacting modes and the dimensionless invariant that selected phase-closed modes in 2D. Otherwise, the 3D system could contain modes with no consistent projection onto any 2D phase-closed configuration, violating dimensional consistency. Hence

$$\frac{V_{sphere}}{V_{lens}} = \pi\sqrt{1-\alpha^2}, \tag{19}$$

$$\therefore \pi\sqrt{1-\alpha^2} = \frac{16}{(5-\sqrt{2}\alpha)(1+\sqrt{2}\alpha)^2}. \tag{20}$$

The equality $V_{sphere}/V_{lens} = \pi'$ is not derived from QED but motivated by a mode-counting consistency argument that can be stated precisely. In 2D, the phase-closure condition $\lambda/D = \pi$ selects, from all possible wave modes on a disk, exactly the subset whose periodicity matches the geometric boundary. The ratio of total modes to selected modes is π. When kinematics are relativistic, this ratio becomes $\pi' = \pi\sqrt{1-\alpha^2}$. In 3D, we identify: total modes $\rightarrow V_{sphere}$ (all standing waves fitting inside radius R), and selected modes $\rightarrow V_{lens}$ (waves simultaneously satisfying boundary conditions on both spheres). The postulate asserts that the mode-selection ratio is the same invariant in both dimensions.

This is a consistency requirement: if the 3D ratio differed from π', one could always find a planar cross-section through the interaction axis for which the projected mode

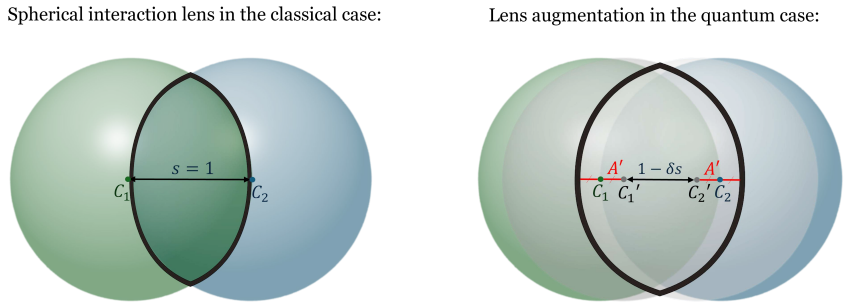


Fig. 2 Left: classical intersection of two spheres with $R = d$. Right: quantum boundary expansion by A', reducing effective separation by $2A'$.

count violated the 2D closure condition. Formally, for any plane Π through the z-axis, the intersection of Π with the lens is a circular segment whose arc-to-chord ratio approaches π' as $s \to 1$. The postulate elevates this planar consistency to a volumetric one.

To verify this embedding explicitly, consider the planar cross-section of the lens at the midpoint $z = d/2$ between the two centers for $s = 1$. The intersection is a circle of radius $r = R\sin 60° = R\sqrt{3}/2$, with circumference $2\pi r = \pi R\sqrt{3}$. To first order, consistency with 2D phase closure requires the effective arc length in any planar section to obey the same relativistic scaling as Eq. (7). We therefore assume, as part of our definition of 3D phase closure, that arcs lying in the lens carry the same effective contraction factor $(1 - \alpha^2/2)$, giving

$$L_{arc} \simeq \pi R\sqrt{3}\,(1 - \alpha^2/2) \simeq \pi' R\sqrt{3}, \tag{21}$$

where we used $\pi' = \pi\sqrt{1-\alpha^2} \simeq \pi(1 - \alpha^2/2)$ exactly as we did in 2D to obtain the Pythagorean relation for the effective perimeter. The chord spanning the lens in this section has length $D_{chord} = R\sqrt{3}$. Hence $L_{arc}/D_{chord} \simeq \pi'$, showing that the 2D invariant is geometrically consistent with every planar cross-section. The volumetric postulate Eq. (20) is the minimal 3D statement that ensures this holds for all sections simultaneously.

This condition is non-trivial: for classical sharp spheres with $s = 1$, $V_{sphere}/V_{lens} = 16/5 = 3.2$, implying too few shared modes for closure. Quantum uncertainty effectively increases the number of potential shared modes, making $s < 1$ by the amount δs, thus increasing the lens volume until the mode ratio matches π'. The ratio α emerges as the finite scaling that renders the subset of interacting 3D modes consistent with 2D phase closure in every orientation simultaneously.

The value of the fine structure constant is not inserted at any point. The role of α in the equation is simply that of the unknown we must solve for. The only geometrically relevant real solution of Eq. (20) (with $0 < s < 2$) is

$$\alpha_1^{-1} = 137.190126082. \tag{22}$$

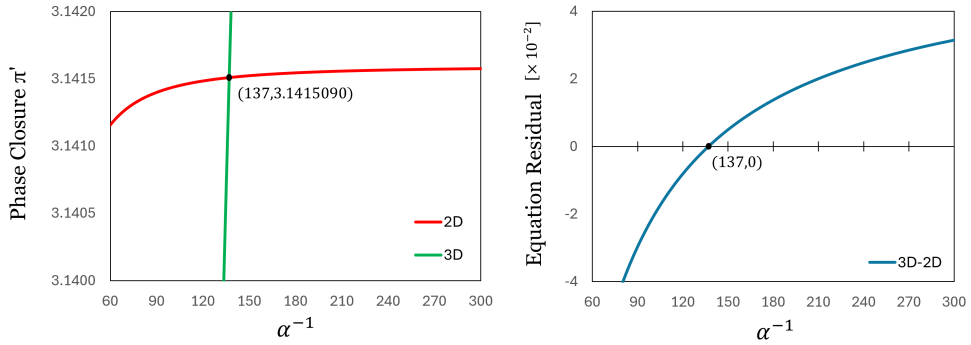


Fig. 3 Solution of Eq. (20). Red: $\pi\sqrt{1-\alpha^2}$; green: volumetric ratio. Crossing and zero residue (blue) give $\alpha_1^{-1} \simeq 137$.

This leading equation for a geometric scaling achieves agreement within 0.11% relative to the determination of the fine structure constant from the electron $g-2$, $\alpha^{-1} = 137.035999166(15)$ (Fan et al. 2023). Therefore, a dimensionless ratio that was uniquely selected by geometry bears a numerical similarity to the electromagnetic coupling constant within the proposed framework. This raises the possibility that $\alpha \triangleq \Delta\dot{r}/v = 2A/\pi R$ may indeed represent a geometric constraint on the fine structure constant, giving the definition of 3D phase closure measurable consequences. Figure 3 shows the solution as the crossing point of the functions representing each side of the equality.

To summarize the epistemological status and clarify next steps, Eq. (20) is a geometric postulate, motivated by 2D-to-3D mode-counting consistency but not derived from QED. Its validation as a geometric constraint for the fine structure constant rests on four quantitative consequences: the demonstrated accuracy of the tree level, the possibility of extensions within the same geometry, consistency with the anomalous magnetic moment of the electron (Schwinger 1948) and the prediction of future higher-resolution measurements.

4 Higher-order corrections from loop geometry

The tree-level condition, Eq. (20), yields $\alpha_1^{-1} = 137.190$, within 0.11% of experiment. The remaining discrepancy reflects that the boundary displacement A' in Eq. (15) treats the quantum phase surface as rigid. Physically the boundary fluctuates: virtual quanta that sample or traverse the intersection lens modify the effective separation s. These corrections are organized as a series whose terms are fixed, one by one, by named elements of the two-sphere geometry and evaluated before Eq. (41) is solved for α.

4.1 Geometric inputs and organization of the expansion

Four quantities follow directly from the $d = R$ configuration with no freedom: the cap solid angle, the cap fraction, the conversion factor that rescales a per-cap contribution

to the full boundary, and the half-opening angle. Three further ingredients are posited but carry no adjustable parameter and are fixed in advance: the per-order suppression $(\alpha/\pi)^n$, the great-circle baseline weight $1/\pi$ that prevents double-counting of the tree-level average, and the Poisson absorption model.

For two spheres of radius R with centers separated by $d = R$, the intersection circle lies in the bisecting plane and subtends a half-opening angle θ_0 at each center with $\cos\theta_0 = (d/2)/R = 1/2$, so $\theta_0 = 60°$. The spherical cap bounding the lens then has solid angle

$$\Omega_{\rm cap} = 2\pi\,(1 - \cos\theta_0) = 2\pi\left(1 - \tfrac{1}{2}\right) = \pi, \tag{23}$$

and the fraction of directions from a center pointing into the lens is

$$f = \frac{\Omega_{\rm cap}}{4\pi} = \frac{1}{4}, \qquad \frac{4\pi}{\Omega_{\rm cap}} = 4 = \frac{1}{f}. \tag{24}$$

The conversion factor $4\pi/\Omega_{\rm cap}$ returns a per-cap fractional contribution to the full boundary; being the exact reciprocal of f, it cancels the cap fraction in every δs_n, a property of the $d = R$ geometry.

Each correction follows the same construction: the raw per-cap contribution $f\,w_n$, with w_n the order-n weight specified below, is reduced by the part a_n already represented at lower order, rescaled to the full boundary, and assigned a sign σ_n,

$$\delta s_n = \sigma_n \frac{4\pi}{\Omega_{\rm cap}}\,(f\,w_n - a_n)\,, \qquad \frac{4\pi}{\Omega_{\rm cap}}\,f = 1. \tag{25}$$

This makes explicit where the subtraction enters; the one-loop and multi-loop terms differ only in their weight, subtraction, sign, and an interchange factor.

The boundary shift is expanded as

$$s = 1 - \delta s, \ \text{ where} \tag{26}$$

$$\delta s = \sum_{n=1}^{\infty} \delta s_n, \qquad \delta s_1 = \sqrt{2}\,\alpha. \tag{27}$$

For $n \geq 2$ each term scales as $(\alpha/\pi)^n$, multiplied by a sign σ_n and a numerical coefficient of order unity that the geometry fixes, so the magnitude falls by $\sim \alpha/\pi$ at each successive order. This scaling is not derived from diagrammatic power counting; it is an assumption of the construction. The weight is $w_2 = \alpha^2/\pi$ for the single-sphere one-loop term and $w_n = (\alpha/\pi)^n$ for the two-sphere terms with $n \geq 3$; in both cases the final term reduces to a coefficient of order unity times $(\alpha/\pi)^n$.

The baseline weight $1/\pi$ is the normalization constant of the uniform tilt measure $d\theta/\pi$ that defines the tree-level average, Eq. (14); the fraction of any cap contribution already represented in δs_1 is taken to equal this constant. It is deliberately distinguished from the projection-weighted mean $2/\pi = (1/\pi)\int_0^\pi \sin\theta\,d\theta$ that sets the amplitude of δs_1. The two are different objects: $2/\pi$ is the expectation value of the z-projection and fixes how large the tree-level displacement is, whereas the double-counting overlap is governed by the flat weight the uniform measure assigns across

orientations, namely its normalization constant $1/\pi$, and not by the magnitude of the averaged projection. This single number governs the removal of double-counting at every order. The sign at one loop is negative, $\sigma_2 = -1$, reflecting the screening of the interaction by vacuum polarization at long distance (Peskin and Schroeder 1995). For $n \geq 3$ we posit an alternating sign $\sigma_n = (-1)^n$, screening for odd n and antiscreening for even n; this alternation is motivated by, but not identical to, the loop-order sign structure of QED vacuum polarization.

4.2 One-loop correction: second order

At one loop, a virtual quantum is emitted from the boundary of sphere 1, samples the lens, and is reabsorbed by sphere 1. Because the quantum returns to its own electron, this is a single-sphere, self-energy-type process: no identical particles are exchanged and no interchange factor arises. Quanta whose worldlines miss the lens renormalize the isolated sphere and leave s unchanged.

The fraction of emitted quanta entering the lens is $f = \Omega_{\text{cap}}/4\pi = 1/4$, and the single-sphere one-loop weight is $w_2 = \alpha^2/\pi$. The raw per-cap contribution is therefore

$$f\, w_2 = \frac{1}{4} \cdot \frac{\alpha^2}{\pi} = \frac{\alpha^2}{4\pi}. \tag{28}$$

Of this, the great-circle baseline already absorbed into δs_1 accounts for the fraction $1/\pi$, so the already-counted piece is

$$a_2 = \frac{1}{\pi} \cdot \frac{\alpha^2}{4\pi} = \frac{\alpha^2}{4\pi^2}, \tag{29}$$

and the new contribution is

$$f\, w_2 - a_2 = \frac{\alpha^2}{4\pi} - \frac{\alpha^2}{4\pi^2} = \frac{(\pi - 1)\,\alpha^2}{4\pi^2}. \tag{30}$$

Applying the conversion $4\pi/\Omega_{\text{cap}} = 4$ multiplied by $(f w_2 - a_2)$ per Eq. (25) cancels the factor four in the denominator, and the screening sign gives

$$\delta s_2 = -(\pi - 1) \left(\frac{\alpha}{\pi}\right)^2. \tag{31}$$

The factor $\pi - 1$ admits a compact reading: expressed in units of $(\alpha/\pi)^2$, the one-loop cap weight equals π and the baseline removes unity.

The same lens geometry reproduces the leading anomalous magnetic moment. In QED, the Schwinger term $a_e = \alpha/2\pi$ arises from the vertex correction (Schwinger 1948). For $s = 1$ the lens subtends $\Omega_{\text{cap}} = \pi$ at each center, so the relevant solid-angle fraction is the same single-center value used for the loop corrections,

$$\frac{\Omega_{\text{cap}}}{4\pi} = \frac{1}{4}. \tag{32}$$

Combining this fraction with the tilt average $(1/\pi)\int_0^\pi \sin\theta\, d\theta = 2/\pi$ already obtained in Eq. (14) and one power of the coupling gives, at first order in α,

$$a_e = \frac{\Omega_{\rm cap}}{4\pi} \times \frac{2}{\pi} \times \alpha = \frac{1}{4} \times \frac{2}{\pi} \times \alpha = \frac{\alpha}{2\pi} = 1.1614 \times 10^{-3}, \tag{33}$$

recovering the Schwinger result. Both numerical factors are quantities already fixed elsewhere in the construction—the cap fraction $\Omega_{\rm cap}/4\pi = 1/4$ that governs the loop corrections and the tilt average $2/\pi$ of Eq. (14)—so no factor is introduced specifically to obtain this result. Equation (33) is a consistency check rather than a derivation: the QED result depends on the photon propagator and the spinor trace structure, which are not reproduced here, while the lens geometry supplies only the same numerical mode-counting performed by the loop integral.

4.3 Multi-loop corrections: third order and beyond

Beyond one loop, the virtual quantum must cross the lens and reach sphere 2. Two features then distinguish these terms from the one-loop case. The process connects two identical electrons and is counted with an interchange factor 1/2 that removes the double-counting of the $(1 \leftrightarrow 2)$ labeling; this factor is absent at one loop precisely because that process returns to a single sphere. The traversal is moreover subject to absorption within the lens.

We model these absorption events as a Poisson process, taking them to be rare, independent, and uniform in rate along the path, the conditions under which the count in a fixed interval is Poisson-distributed. At $d = R$ a single intersection lens lies between the spheres, so a direct traversal crosses one lens per interaction cycle and the mean number of absorption opportunities is $\mu = 1$, fixed by the geometry and free of any length scale. The probability of reaching sphere 2 with no intermediate absorption is the Poisson zero-count probability

$$P_{\rm transmit} = e^{-\mu} = e^{-1}. \tag{34}$$

Thus e enters from the statistics of lens traversal as π entered from the isotropic averaging of planar modes, each fixed by the two-sphere geometry.

With the order-n weight $w_n = (\alpha/\pi)^n$, the raw per-cap contribution at third order is

$$f\, w_3 = \frac{1}{4}\left(\frac{\alpha}{\pi}\right)^3. \tag{35}$$

The already-counted piece is the part that both overlaps the great-circle baseline, weight $1/\pi$, and survives traversal, weight e^{-1}, so its weight is $1/(e\pi)$ and

$$a_3 = \frac{1}{e\pi}\, f\, w_3 = \frac{1}{4e\pi}\left(\frac{\alpha}{\pi}\right)^3. \tag{36}$$

The new contribution is

$$f\, w_3 - a_3 = \frac{1}{4}\left(1 - \frac{1}{e\pi}\right)\left(\frac{\alpha}{\pi}\right)^3, \tag{37}$$

and applying the conversion factor four, the interchange factor $1/2$, and the screening sign $\sigma_3 = -1$ yields

$$\delta s_3 = -\frac{1}{2}\left(1 - \frac{1}{e\pi}\right)\left(\frac{\alpha}{\pi}\right)^3. \tag{38}$$

A third traversal corresponds to three-loop diagrams. The geometry is unchanged, so $\mu = 1$ and $P_{\text{transmit}} = e^{-1}$, the subtraction weight remains $1/(e\pi)$ and the net factor $1 - 1/(e\pi)$, the weight is now $(\alpha/\pi)^4$, and the interchange factor $1/2$ still applies; the sign becomes $\sigma_4 = +1$, antiscreening,

$$\delta s_4 = +\frac{1}{2}\left(1 - \frac{1}{e\pi}\right)\left(\frac{\alpha}{\pi}\right)^4. \tag{39}$$

The construction repeats unchanged at every higher order,

$$\delta s_n = \frac{(-1)^n}{2}\left(1 - \frac{1}{e\pi}\right)\left(\frac{\alpha}{\pi}\right)^n, \qquad n \geq 3, \tag{40}$$

so that $\frac{1}{2}\left(1 - 1/(e\pi)\right)$ is common to all orders $n \geq 3$, the sign alternating between screening for odd n and antiscreening for even n, and the magnitude falling by $\sim \alpha/\pi$ at each step. The one-loop term stands apart from Eq. (40): its coefficient $\pi - 1$ is set by the baseline subtraction alone, the second-order process being confined to a single sphere, whereas the terms with $n \geq 3$ are two-sphere traversals carrying both the transmission and the interchange factors. This is a structural distinction between self-energy and exchange contributions.

4.4 Complete equation and numerical evaluation

Inserting $s = 1 - \sum_{n=1}^{4} \delta s_n$ into the volumetric ratio gives the phase-closure condition

$$\pi\sqrt{1 - \alpha^2} = \frac{16}{(5 - \delta s)\,(1 + \delta s)^2}, \tag{41}$$

with

$$\delta s = \sqrt{2}\,\alpha - (\pi - 1)\,\frac{\alpha^2}{\pi^2} - \frac{1}{2}\left(1 - \frac{1}{e\pi}\right)\frac{\alpha^3}{\pi^3} + \frac{1}{2}\left(1 - \frac{1}{e\pi}\right)\frac{\alpha^4}{\pi^4}. \tag{42}$$

Every coefficient in Eq. (42)—the $\sqrt{2}$ of the rms projection and tilt average of Sec. 3.2, the $\pi - 1$ of the one-loop cap-minus-baseline subtraction, the $1/2$ of interchange symmetry, and the e^{-1} of Poisson transmission—is fixed by the two-sphere geometry before Eq. (41) is solved.

Table 1 lists the solution at each order. The term δs_1 alone gives a relative error of 1.12×10^{-3}; adding δs_2 reduces it to 5.38×10^{-7}, δs_3 to 1.17×10^{-9}, and δs_4 to 8.03×10^{-11}, an agreement of 0.7σ with the independent $g-2$ determination (Fan et al. 2023). The table records the stability of a fixed series under the successive inclusion of geometrically determined terms.

Table 1 Stability of the phase-closure solution. Each term is fixed by the same two-sphere geometry prior to solving for α. Relative errors are referred to the determination of α from the electron magnetic moment $(g-2)$ (Fan et al. 2023), reaching 0.7σ at fourth order.

Separation Term $\delta s_n(\alpha)$	**Calculated** α^{-1}	**Relative Error**
Electron $g-2$ (Fan et al. 2023)	137.035999166(15)	—
$\delta s_1 = \sqrt{2}\alpha$	137.190126082	1.12×10^{-3}
$\delta s_2 = -(\pi - 1)\,\dfrac{\alpha^2}{\pi^2}$	137.036072851	5.38×10^{-7}
$\delta s_3 = -\dfrac{1}{2}\left(1 - \dfrac{1}{e\pi}\right)\dfrac{\alpha^3}{\pi^3}$	137.035999006	1.17×10^{-9}
$\delta s_4 = +\dfrac{1}{2}\left(1 - \dfrac{1}{e\pi}\right)\dfrac{\alpha^4}{\pi^4}$	137.035999177	8.03×10^{-11} (0.7σ)

We do not claim the series terminates at $n = 4$ or that further terms vanish. Rather, Eq. (42) is consistent with the experimental value to the limit of present precision. Including δs_5 shifts α^{-1} from 137.0359991772 to 137.0359991768, a change of -4.0×10^{-10}, indistinguishable within current uncertainty. This yields a rigid two-tier prediction. A future measurement with absolute uncertainty 10^{-9} is expected to report $\alpha^{-1} = 137.035999177$; values outside the interval [137.035999172, 137.035999182] would falsify the series at that precision. At resolution 10^{-10} the series predicts $\alpha^{-1} = 137.0359991768$; values outside [137.0359991763, 137.0359991773] would falsify it. These intervals carry no adjustable freedom, since the coefficients cannot be modified without violating the baseline, transmission, or interchange rules of Sec. 4.1.

Finally, the prediction must be read against a current experimental situation in which the most precise determinations of α do not agree. The determination from the electron magnetic moment $(g-2)$, $\alpha^{-1} = 137.035999166(15)$ (Fan et al. 2023), is the most precise value independent of the atomic-recoil technique, and the geometric prediction agrees with it at 0.7σ. The two recoil determinations are themselves mutually discrepant at $\sim 5.5\sigma$: photon-recoil interferometry on ^{133}Cs gives $\alpha^{-1} = 137.035999046(27)$ (Parker et al. 2018), whereas the same technique on ^{87}Rb gives $\alpha^{-1} = 137.035999206(11)$ (Morel et al. 2020). The geometric value lies between them, $\sim 2.6\sigma$ below the rubidium value and $\sim 5\sigma$ above the cesium value, and coincides with the CODATA 2022 recommended mean $\alpha^{-1} = 137.035999177(21)$ (Tiesinga et al. 2024), whose uncertainty is driven by precisely this unresolved recoil discrepancy. Since the two recoil results are mutually inconsistent, no single measurement can presently confirm or exclude the series. The construction makes a definite directional

commitment: it predicts that improved recoil determinations should converge toward the prediction near 137.0359991768, agreeing with the $g-2$ value and coinciding with the CODATA 2022 mean, rather than toward either current recoil central value.

5 Effective field theory framing

Given the geometric postulate of Eq. (20), we show that it admits a consistent embedding within low-energy effective field theory (EFT) using a hard-sphere spatial regulator. We do not claim that QED uniquely selects this regulator or that the postulate is derivable from QED. The purpose is to demonstrate that the construction can be expressed in the language of quantum field theory without obstruction.

5.1 Hard-sphere regulator and mode counting

Hard-sphere boundary conditions as spatial regulators appear in several established contexts: the Casimir effect, where conducting-boundary conditions define the mode spectrum (Casimir 1948; Milton 2001); non-relativistic EFT for nucleon-nucleon scattering with hard-core potentials (Kaplan et al. 1998; van Kolck 1999); and lattice field theory, where a spatial cutoff at scale R suppresses modes with $k \gtrsim \pi/R$ (Montvay and Münster 1994). The common feature is that the number of modes available below a momentum cutoff $k_{\max}$ in a spherical volume of radius R scales as

$$N_{\text{modes}} \sim \frac{V_{\text{sphere}}\, k_{\max}^3}{6\pi^2} \propto V_{\text{sphere}}, \tag{43}$$

so that the ratio of mode counts between two domains equals their volume ratio. This is the standard result underlying the Casimir energy density (Milton 2001), and it justifies identifying the ratio of mode counts with the volume ratio $V_{\text{sphere}}/V_{\text{lens}}$, i.e. $Z_i \propto V_{\text{sphere}}$. We stress what this does and does not fix: it determines the mode-count ratio, while the further identification of that ratio with $\pi\sqrt{1-\alpha^2}$ is the postulate of Eq. (19), and the order-by-order weights w_n of Sec. 4.1 enter as separate inputs not supplied by Eq. (43).

5.2 EFT rewriting of the phase-closure condition

Consider two electron fields ψ_1, ψ_2 separated by d. Define for each a spatial domain $\mathcal{D}_i = \{\mathbf{x} : |\mathbf{x} - \mathbf{x}_i| \le R\}$ with $R = d$. Impose Dirichlet boundary conditions $\psi_i = 0$ on $\partial\mathcal{D}_i$ for modes with wavelength $\lambda \gtrsim R$; this is the hard-sphere regulator used in nuclear EFT (Kaplan et al. 1998). A hard cutoff at fixed R does not preserve exact Lorentz invariance, since lengths contract under boosts; R is therefore defined in the rest frame of the two-electron system, and boost invariance is recovered only approximately, at the non-relativistic scales relevant here (Lepage 1997).

The free partition function for each field is $Z_i \propto V_{\text{sphere}}$ by Eq. (43). The interaction couples only modes supported in the overlap $\mathcal{D}_1 \cap \mathcal{D}_2$, giving $Z_{\text{int}} \propto V_{\text{lens}}$. The effective action contains

$$S_{\text{eff}} \supset \int d^4x\, \psi_1^\dagger \psi_1\, \psi_2^\dagger \psi_2\, \frac{V_{\text{lens}}}{V_{\text{sphere}}}\, g_0, \tag{44}$$

with g_0 the bare coupling. The renormalization condition that the effective coupling measured at separation R equals the 2D relativistic phase invariant gives

$$\frac{V_{\text{sphere}}}{V_{\text{lens}}} = \pi\sqrt{1-\alpha^2}, \tag{45}$$

identical to Eq. (19). This is structurally analogous to renormalization conditions in dimensional regularization (t Hooft 1973; Collins 1984), where finite parts of renormalized couplings are fixed by the geometry of the regularization scheme; here the coupling is fixed by the geometry of the intersection lens rather than the dimension of spacetime.

5.3 Scope and limitations

The EFT rewriting shows that the geometric framework is expressible in quantum-field-theoretic language with no obstruction. A genuinely independent test would be diagrammatic: evaluating the two-loop vacuum-polarization contribution with Dirichlet boundary conditions at radius R and extracting the third-order coefficient of $(\alpha/\pi)^3$, which the construction predicts to be $\frac{1}{2}(1-1/e\pi)$. Such a computation would not reuse the geometric inputs of Sec. 4 and would therefore test that coefficient independently; it remains a natural next step.

A final point in terms of scope is the energy dependence of the coupling. Throughout this work, α denotes the fine structure constant in the Thomson zero-momentum-transfer limit, the low-energy value determined by the electron-anomaly and atomic-recoil programs. The construction fixes this single infrared value; it does not describe the running of the coupling, whereby α increases with momentum transfer and α^{-1} falls to $\alpha^{-1}(M_Z) \simeq 128$ at the scale of the Z boson (Gell-Mann and Low 1954; Peskin and Schroeder 1995). In QED, the renormalization group fixes how α evolves with scale but takes the infrared value as a boundary condition that the theory does not itself predict; it is precisely this undetermined boundary value that the present geometry constrains. The hard-sphere regulator of this section and the long-distance screening that organizes the corrections of Sec. 4 are likewise infrared statements, so the entire construction is internally confined to the low-energy regime. A geometric account of the scale dependence itself, if possible, requires promoting the fixed sphere radius $R = d$ to a scale-dependent quantity and lies beyond the present scope.

6 Conclusion

We have proposed a minimal definition for three-dimensional phase closure. We modeled an interaction geometrically through two spheres of influence whose radii equal the particles' separation (excluding any external length). Treating the system quantum-relativistically while requiring cross-dimensional consistency reveals a characteristic geometric scaling. The numerical solution naturally points to a connection with the fine structure constant. The leading result $\alpha_1^{-1} \simeq 137.19$ comes from the coefficient $\sqrt{2}$, which arises from the rms projection of the phase-closed orbit onto the interaction

axis averaged over the single rotational degree of freedom introduced by the 3D promotion, Eq. (15). We do not derive the sphere postulate from QED; we show that if it is accepted, the value of α can be constrained by the consistency condition Eq. (19). Higher-order coefficients are modeled from solid-angle overlaps of spherical caps, the Poisson transmission rule, and interchange symmetry within the same geometry.

The present construction differs fundamentally from Wyler's 1969 approach (Wyler 1969) in both epistemology and geometry. Wyler obtained α^{-1} from volumes of homogeneous domains $SO(5,1)/SO(5) \times SO(1,1)$ associated with the conformal group, reproducing the experimental value to 6 digits. However, as Robertson (Robertson 1971) and Adler (Adler 1972) demonstrated, the result depended on ad hoc identifications: choosing $SO(7)$ or a different embedding yields unrelated numbers. Crucially, Wyler's domains are 5-complex-dimensional manifolds; their physical reality requires extra dimensions that have never been observed, making the construction empirically untestable beyond the single number it fits.

By contrast, the sphere-lens geometry is formulated entirely in ordinary 3D Euclidean space. No higher dimensions, compactifications, or unobservable structures are invoked. The spheres represent regions of influence defined by the separation d between two electrons, and therefore carry a relational meaning rather than representing fixed physical boundaries or introducing independent length scale. Consequently, validation does not require introducing additional degrees of freedom beyond those already associated with 3D space and quantum phase closure. The geometry is thus both minimal and empirically accessible.

The observed numerical agreement reinforces this conceptual distinction. Wyler's formula gave $\alpha^{-1} = 137.03608$, an error of 8×10^{-7}. The present tree-level result $\alpha_1^{-1} = 137.190$ is already within 1.1×10^{-3}, and the fourth-order series yields $\alpha_4^{-1} = 137.035999177$, agreeing with the determination of α from the electron $g-2$ within a relative deviation of 8×10^{-11}. The improvement over Wyler's six-figure agreement by four orders of magnitude is not incremental: it reaches the level of precision at which QED radiative corrections become relevant, suggesting the lens coefficients may reflect a structure comparable to that of loop corrections. Moreover, the same geometry is consistent with the Schwinger term $a_e = \alpha/2\pi$, Eq. (33), while Wyler's framework lacks contact with a second number.

The model can be viewed as a geometric regulator that constrains the value of α by enforcing 3D phase coherence, as dimensional regularization selects finite parts in QED. The advantage of a simple 3D geometry over 5-complex-dimensional groups suggests that α may belong to the same category as π or $\sqrt{2}$: a dimensionless constant whose value is associated with geometric consistency. Whether this framework is ultimately correct is a question experiment can now address directly.

Eq. (40) provides a sharp test. The fifth-order term $\delta s_5 = -\frac{1}{2}(1 - 1/e\pi)\alpha^5/\pi^5$ shifts α^{-1} at the 10^{-10} level, currently below experimental resolution. A rigid two-tier prediction follows: a future experiment with absolute uncertainty of 10^{-9} should report a result within $\alpha^{-1} = 137.035999177(5)$; at resolution 10^{-10}, the series predicts $\alpha^{-1} = 137.0359991768(5)$. Values outside either interval would falsify the series at the respective precision, since the coefficients cannot be modified without violating the baseline, transmission, or interchange rules. At present, the predicted value agrees with

the determination from the electron $g-2$ at 0.7σ level and coincides with the CODATA 2022 recommended mean, lying between the mutually discrepant cesium and rubidium recoil measurements; the construction therefore makes a definite directional commitment: improved recoil determinations should converge toward $\alpha^{-1} \simeq 137.0359991768$ rather than toward either present recoil value. Thus, the 3D phase-closure model is not only more parsimonious than Wyler's, but also more predictive, making direct contact with an open question at the frontier of precision metrology.

Acknowledgments. The author would like to thank A.L.B.R. for the encouragement and candidness.

Data availability. No datasets were generated or analyzed during the current study.

Competing interests. The author declares no competing interests.

References

Adler, S.L.: Theories of the Fine Structure Constant. Technical Report 72/059-T, Fermilab (1972)

Bronnikov, K.A., Ivashchuk, V.D., Khruschov, V.V.: The Fine-Structure Constant: A Review of Measurement Results and Possible Space-Time Variations. Measurement Techniques **68**, 125–134 (2025)

Bohr, N.: On the Constitution of Atoms and Molecules. Philosophical Magazine **26**(151), 1–25 (1913)

Barrow, J.D., Tipler, F.J.: The Anthropic Cosmological Principle. Oxford University Press, Oxford (1986)

Casimir, H.B.G.: On the attraction between two perfectly conducting plates. Proc. Kon. Ned. Akad. Wet. **51**, 793–795 (1948)

Candelas, P., Horowitz, G.T., Strominger, A., Witten, E.: Vacuum configurations for superstrings. Nucl. Phys. B **258**, 33–74 (1985)

Collins, J.C.: Renormalization. Cambridge University Press, Cambridge (1984)

Dirac, P.A.M.: The Quantum Theory of the Electron. Proc. Roy. Soc. A **117**, 610–624 (1928)

Eddington, A.S.: The Constants of Nature. Cambridge University Press, Cambridge (1931)

Eddington, A.S.: Relativity Theory of Protons and Electrons. Cambridge University Press, Cambridge (1936)

Einstein, A.: Autobiographical Notes. In: Schilpp, P.A. (ed.) Albert Einstein: Philosopher-Scientist, pp. 1–95. Library of Living Philosophers, Evanston, Illinois (1949)

Feynman, R.P.: QED: The Strange Theory of Light and Matter. Princeton University Press, Princenton, NJ (1985)

Fan, X., Myers, T.G., Sukra, B.A.D., Gabrielse, G.: Measurement of the electron magnetic moment. Phys. Rev. Lett. **130**(7), 071801 (2023)

Gell-Mann, M., Low, F.E.: Quantum Electrodynamics at Small Distances. Phys. Rev. **95**, 1300–1312 (1954)

Griffiths, D.J., Schroeter, D.F.: Introduction to Quantum Mechanics, 3rd edn. Cambridge University Press, Cambridge (2018)

Heath, T.L.: The Thirteen Books of Euclid's Elements. Dover Publications, New York (1956)

Hanneke, D., Fogwell, S., Gabrielse, G.: New Measurement of the Electron Magnetic Moment and the Fine Structure Constant. Phys. Rev. Lett. **100**, 120801 (2008)

Jackson, J.D.: Classical Electrodynamics, 3rd edn. Wiley, New York (1999)

Jentschura, U.D., Nándori, I.: Attempts at a determination of the fine-structure constant from first principles: A brief historical overview. The European Physical Journal H **39**(5), 591–611 (2014)

Kragh, H.: Magic Number: A Partial History of the Fine-Structure Constant. Arch. Hist. Exact Sci. **57**, 395–431 (2003)

Kaplan, D.B., Savage, M.J., Wise, M.B.: A new expansion for nucleon-nucleon interactions. Phys. Lett. B **424**, 390–396 (1998)

Lang, S.: Introduction to Arakelov Theory. Springer, New York (1988)

Lepage, G.P.: How to renormalize the Schrödinger equation. Nuclear Physics B (Proc. Suppl.) (1997)

Milton, K.A.: The Casimir Effect: Physical Manifestations of Zero-Point Energy. World Scientific, Singapore (2001)

Montvay, I., Münster, G.: Quantum Fields on a Lattice. Cambridge University Press, Cambridge (1994)

Mohr, P.J., Newell, D.B., Taylor, B.N.: CODATA Recommended Values of the Fundamental Physical Constants. Rev. Mod. Phys. **88**, 035009 (2016)

Morel, L., Yao, Z., Cladé, P., Guellati-Khélifa, S.: Determination of the fine-structure constant with an accuracy of 81 parts per trillion. Nature **588**(7836), 61–65 (2020)

Pauli, W.: Exclusion Principle and Quantum Mechanics. Elsevier Publishing Company, Amsterdam (1946). Nobel Lecture, December 13, 1946

Pauli, W.: Ideas of the Field Structure of Matter. Rev. Mod. Phys. **27**, 1–14 (1955)

Peskin, M.E., Schroeder, D.V.: An Introduction to Quantum Field Theory. Addison-Wesley, Reading, MA (1995)

Parker, R.H., Yu, C., Zhong, W., Estey, B., Müller, H.: Measurement of the fine-structure constant as a test of the Standard Model. Science **360**(6385), 191–195 (2018)

Robertson, B.: Wyler's Expression for the Fine-Structure Constant. Phys. Rev. Lett. **27**, 1545–1547 (1971)

Schwinger, J.: On Quantum-Electrodynamics and the Magnetic Moment of the Electron. Phys. Rev. **73**, 416–417 (1948)

Sommerfeld, A.: Zur Quantentheorie der Spektrallinien. Annalen der Physik **356**, 1–94 (1916)

Sommerfeld, A.: Atomic Structure and Spectral Lines. Methuen & Co., London (1923)

Hooft, G.: Dimensional regularization and the renormalization group. Nuclear Physics B **61**, 455–468 (1973)

Tiesinga, E., Newell, D.B., Mohr, P.J., Taylor, B.N.: CODATA Recommended Values of the Fundamental Physical Constants: 2022. J. Phys. Chem. Ref. Data **53** (2024)

Kolck, U.: Effective field theory of nuclear forces. Prog. Part. Nucl. Phys. **43**, 337–418 (1999)

Weinberg, S.: The cosmological constant problem. Reviews of Modern Physics **61**, 1 (1989)

Weinberg, S.: Living in the Multiverse. In: Carr, B. (ed.) Universe or Multiverse?, pp. 29–42. Cambridge University Press, Cambridge (2007)

Wyler, A.: L'espace symétrique du groupe des équations de Maxwell. C. R. Acad. Sci. Paris A **269**, 743–745 (1969)